



Warming slowdown over the Tibetan plateau in recent decades

Yaojie Liu^{1,2} · Yangjian Zhang^{1,2,3} · Juntao Zhu¹ · Ke Huang^{1,2} · Jiaxing Zu^{1,2} · Ning Chen^{1,2} · Nan Cong¹ · Annemiek Irene Stegehuis⁴

Received: 6 July 2017 / Accepted: 20 February 2018 / Published online: 10 March 2018
© Springer-Verlag GmbH Austria, part of Springer Nature 2018

Abstract

As the recent global warming hiatus and the warming on high elevations are attracting worldwide attention, this study examined the robustness of the warming slowdown over the Tibetan plateau (TP) and its related driving forces. By integrating multiple-source data from 1982 to 2015 and using trend analysis, we found that the mean temperature (T_{mean}), maximum temperature (T_{max}) and minimum temperature (T_{min}) showed a slowdown of the warming trend around 1998, during the period of the global warming hiatus. This was found over both the growing season (GS) and non-growing season (NGS) and suggested a robust warming hiatus over the TP. Due to the differences in trends of T_{max} and T_{min} , the trend of diurnal temperature range (DTR) also shifted after 1998, especially during the GS temperature. The warming rate was spatially heterogeneous. The northern TP (NTP) experienced more warming than the southern TP (STP) in all seasons from 1982 to 1998, while the pattern was reversed in the period from 1998 to 2015. Water vapour was found to be the main driving force for the trend in T_{mean} and T_{min} by influencing downward long wave radiation. Sunshine duration was the main driving force behind the trend in T_{max} and DTR through a change in downward shortwave radiation that altered the energy source of daytime temperature. Water vapour was the major driving force for temperature change over the NTP, while over the STP, sunshine duration dominated the temperature trend.

Keywords Tibetan plateau · Warming hiatus · Land surface temperature · MODIS · Mann-Kendall

Electronic supplementary material The online version of this article (<https://doi.org/10.1007/s00704-018-2435-3>) contains supplementary material, which is available to authorized users.

✉ Yangjian Zhang
zhangyj@igsnr.ac.cn

Yaojie Liu
liuyj.14b@igsnr.ac.cn

Juntao Zhu
zhujt@igsnr.ac.cn

Ke Huang
huangk.13b@igsnr.ac.cn

Jiaxing Zu
zujx.15b@igsnr.ac.cn

Ning Chen
chenn.16b@igsnr.ac.cn

Nan Cong
Congnan@igsnr.ac.cn

Annemiek Irene Stegehuis
stegehuis@pkusz.edu.cn

¹ Lhasa Plateau Ecosystem Research Station, Key Laboratory of Ecosystem Network Observation and Modeling, Institute of Geographic Sciences and Natural Resources Research, Chinese Academy of Sciences, Beijing 100101, China

² College of Resources and Environment, University of Chinese Academy of Sciences, Beijing 100190, China

³ Center for Excellence in Tibetan Plateau Earth Sciences, Chinese Academy of Sciences, Beijing 100101, China

⁴ Shenzhen Key Laboratory of Circular Economy, School of Urban Planning and Design, Shenzhen Graduate School, Peking University, Shenzhen 518055, China

1 Introduction

The global mean temperature has increased with approximately 0.85 K from 1880 to 2012 (IPCC 2013). However, since Easterling and Wehner demonstrated an absence of warming of the global averaged surface air temperature for the period 1998 to 2008 (Easterling and Wehner 2009), the global warming slowdown has been widely discussed (Fyfe et al. 2013a, 2016; Hedemann et al. 2017; Kaufmann et al. 2011; Kosaka and Xie 2013; Meehl et al. 2011; Trenberth et al. 2014). Decreased stratospheric water vapour concentrations have been suggested to slow the global surface temperature increase by approximately 25% from 2000 to 2009 (Solomon et al. 2010). Several studies consider the warming hiatus to be a common climate phenomenon caused by the heat uptake of the deep ocean (Fyfe et al. 2013a; Guemas et al. 2013; Kosaka and Xie 2013; Meehl et al. 2011). Other possible reasons for the warming hiatus could be reduced radiative forcing, cloud cooling or observational errors (Cowtan and Way 2014; Fyfe et al. 2013a, b; Haywood et al. 2014; Hedemann et al. 2017; Karl et al. 2015; Mauritsen 2016; Mears et al. 2011; Morice et al. 2012; Santer et al. 2014; Smith et al. 2016; Solomon et al. 2011).

Mounting evidence suggests that the rate of warming increases with elevation, such that high mountains and plateaus experience greater warming than lower elevations (Pepin et al. 2015). Land surface albedo feedbacks, blackbody emission, clouds, water vapour and aerosols all change with elevation and their elevation-dependent patterns can affect the warming trend along the elevation (Liu et al. 2009; Naud et al. 2012; Rangwala et al. 2010; Ruckstuhl et al. 2007; Tian et al. 2014; Yan et al. 2016; Zhou et al. 2007). In addition, most of the atmospheric loading of aerosol pollutants is located at relatively low elevations, which decreases the flux of shortwave radiation in these regions, known as the surface dimming effect (Tudoroiu et al. 2016; Zeng et al. 2015). Considering these differences, it is necessary to explore the climate warming trend at high elevations and evaluate whether the warming hiatus exist here as well.

The Tibetan plateau (TP) is the highest and most extensive plateau in the world and has long been called the ‘roof of the world’. It covers about 2.5 million km², of which 1.4 million km², or 56% of the total area, is at more than 4000 m above sea level (Zhang et al. 2002). Climate change in this region plays a key role for both regional and global climate through thermal and mechanical forcing (An et al. 2001). The TP is regarded as one of the most sensitive areas for global change (Piao et al. 2012; Zhang et al. 2013), and the warming rate in this region has exceeded that of the northern hemisphere and the region’s latitudinal zone in the recent decades (Zhong et al. 2011). Several studies reported that the significant warming is constant and that there is no warming slowdown over the TP (Cai et al. 2017; Duan and Xiao 2015; You et al.

2016). Even an accelerated warming has been suggested after 1998 due to snow ice-albedo feedbacks (You et al. 2016) and cloud-radiation feedbacks (Duan and Xiao 2015). Over a longer time period, a possible recent warming hiatus has been detected by An et al., based on ice core records over the northwestern TP (An et al. 2016). Being one of the most sensitive areas for global change, clarifying whether the warming slowdown or hiatus happened on the TP has regional and global significance.

Previous related studies mostly relied on surface meteorological station records, reanalyses data, numerical climate models and remote sensing products (Cai et al. 2017; Duan and Xiao 2015; Gao et al. 2015; Tao et al. 2014; You et al. 2016; Zeng et al. 2015). Surface meteorological station records are the most frequently used and dependable data, covering a longer time period than, for example, remote sensing data, but they are limited by their sparse distribution on the western TP (Cai et al. 2017). Reanalysis data has been widely used for the last two decades, but it has a known bias compared to station records, mainly because of differences in topographical height and station aspect and slope (You et al. 2013). Remote sensing products are comparable with meteorological station datasets in their accuracy and are more representative in mountainous regions, but have the apparent drawback of their relatively short time span (Cai et al. 2017; Qin et al. 2009; Tao et al. 2014; Zhang et al. 2016a, b).

In this study, both meteorological records and remotely sensed products from moderate resolution imaging spectroradiometer (MODIS) land surface temperature (LST) with a high spatial resolution were used to explore the climate warming patterns on the TP. The objective of this study was twofold: (1) to assess whether there exists a warming slowdown or hiatus on the Tibetan Plateau in the past decades and (2) to investigate the potential regional driving forces behind this phenomenon.

2 Methods

2.1 Data

The period of a ‘year’ was defined from the beginning of the previous winter (December) till the end of the autumn (November). Furthermore, the growing season (GS) was set from May to September, and the non-growing season (NGS) from the previous October to April.

2.1.1 Meteorological data

The China Meteorological Administration (CMA) maintains 106 field stations on the TP. We used the average daily mean, maximum and minimum air temperature (T_{air}) records from 80 stations located on the plateau and calculated their monthly averages. These stations had no

missing data between 1981 and 2015 (<http://data.cma.cn/>). Other meteorological variables such as wind speed, precipitation, sunshine duration and vapour pressure, were also obtained from the CMA data (Fig. 1).

2.1.2 MODIS LST data

The Terra and Aqua MODIS platform provides remote sensing data for large-scale ecological applications. Several types of LST products with different temporal (daily, 8-day and monthly) and spatial ($1 \text{ km} \times 1 \text{ km}$, $0.05^\circ \times 0.05^\circ$ and $5 \text{ km} \times 5 \text{ km}$) resolutions are available (Wan and Dozier 1996). To temporally match the daytime LST data with the data of T_{air} , we chose to use the Aqua platform. Its passing time is 1330 hours local solar time. We used level 3 data, version-5, MYD13A2, with the 8-day passing time and a horizontal resolution of 1 km from 2003 to 2015 (<https://ladsweb.nascom.nasa.gov/>).

2.2 Statistical analyses

The poor-quality data of the MODIS LST products were first removed using a cloud mask. Afterwards, it was interpolated using the harmonic analysis algorithm Harmonic Analysis of Time Series (HANTS) to fill the cloud-affected values (Xu et al. 2013) and averaged over the growing season. The HANTS algorithm applies a least squares curve fitting procedure based on harmonic components by considering the most important frequencies in the time profiles. The fitted curve in the HANTS transform is described as follows:

$$y(t) = a_0 + \sum_{i=1}^N a_i \cos(\omega_i t - \theta_i) \quad (1)$$

where $y(t)$ is the value of the fitted curve at time t , a_0 is the average value of the time series, N is the number of harmonics, a_i is the amplitude of harmonic i , ω_i is the frequency of harmonic i and θ_i refers to the phase of harmonic i (Roerink et al. 2000).

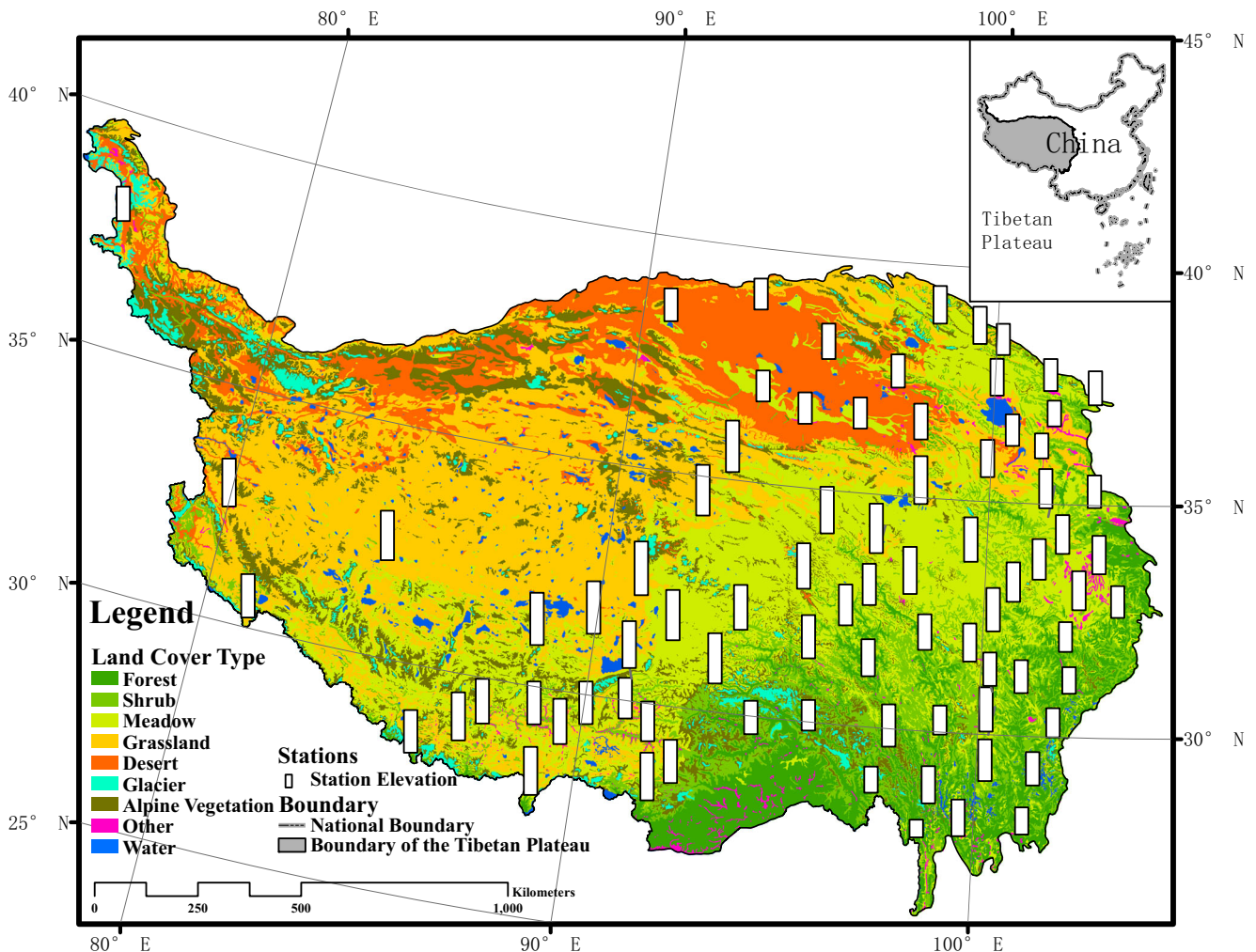


Fig. 1 Distribution of 80 meteorological stations over the Tibetan Plateau. The height of each column reflects the elevation of each station. The different colours represent different land cover types

To calculate the magnitude of the trend of all meteorological variables, the time series was smoothed using a 5-year moving average. We also performed the calculation without smoothing in the supplementary material (similar results were obtained). Afterwards, a linear regression model was used to obtain the warming rate:

$$y = a + bx + e \quad (2)$$

where y , x , e , a and b denote temperature (near-surface air temperature or LST), time (in years), error, intercept and slope (warming rate), respectively. The regression parameters a and b were determined by least-square fitting. The statistical significance of the warming rate was evaluated using the two-tailed Student's t test:

$$t = r[(n-1)/(1-r^2)]^{1/2} \quad (3)$$

where n and r are the total number of years and the correlation coefficient between x and y , respectively.

The Mann-Kendall trend test (Kendall 1955; Mann 1945), one of the most widely used non-parametric tests for detecting trends in time series, was applied to analyse the change in temperature trend. We used the test to evaluate whether the temperature trend changed within the 34-year period on the TP.

To avoid spurious regressions, the detrended original time series was used to estimate the relationships between changes in temperature and changes in precipitation, sunshine duration, and vapour pressure using a multiple linear regression model. First, a correlation analysis was conducted between the detrended temperature data and the four other detrended meteorological variables to evaluate how the different variables affect the possible changes in temperature. Then, a multivariate linear regression model was used to identify the primary factor acting on the trends of T_{\min} , T_{\max} , T_{mean} and diurnal temperature range (DTR). Finally, the spatial pattern of the magnitude of the correlation between temperature and this factor was analysed.

3 Results

3.1 Temperature trends

Annual temperature significantly increased on the TP from 1982 to 2015, based on meteorological station observations (Fig. 2, Fig. S1, Table S1). During the GS, the night and daytime temperatures increased significantly, with a mean rate of 0.05 K/year ($T_{\min, \text{trend}}$) and 0.043 K/year ($T_{\max, \text{trend}}$), respectively (Fig. 2b, Table S1). Because T_{\min} increased more than T_{\max} , the DTR during the GS significantly decreased with a mean rate (DTR_{trend}) of -0.007 K/year (Fig. 2b, Table S1).

During the NGS, the DTR_{trend} was not significant because $T_{\min, \text{trend}}$ (0.052 K/year, significant) was lower than $T_{\max, \text{trend}}$ (0.056 K/year, significant) (Fig. 2c, Table S1). The Mann-Kendall test showed a slowdown of the warming trend from 1998 ($p < 0.05$) (Fig. 2d–f).

Because of the transition in the trend in 1998 (Fig. 2d–f), the temperature trend was investigated separately for periods prior to 1998 and post-1998. During 1982 to 1998, the annual mean, night- and daytime temperature increased with 0.049 K/year ($T_{\text{mean, trend}}$), 0.057 K/year ($T_{\min, \text{trend}}$) and 0.047 K/year ($T_{\max, \text{trend}}$), respectively (Fig. 2a, Table S1). For the same period, the GS mean, night and daytime temperatures increased with similar magnitudes of approximate 0.06 K/year (Fig. 2b, Table S1). The NGS $T_{\text{mean, trend}}$ was 0.028 K/year, which was mainly caused by nighttime warming with a rate of 0.044 K/year ($T_{\min, \text{trend}}$). The trend of daytime warming was 0.015 K/year ($T_{\max, \text{trend}}$) but not significant (Fig. 2c, Table S1).

Since 1998, the climate warming slowed down and the annual trend weakened to 0.021 K/year (Fig. 2a, Table S1). From 2003 to 2015, both remote sensing and meteorological station data were available. In their overlapping period, the remote sensing data showed a significant positive trend of 0.026 K/year (Fig. 2a, Table S1). This slowdown of the annual warming was primarily a result of both a decreased magnitude of GS warming (0.036 K/year, significant) and an absence of trend in the NGS. These results were observed both in the meteorological station data and in the remote sensing data (Fig. 2b, c, Table S1). During the GS, the positive daytime temperature trend ($T_{\max, \text{trend}} = 0.047$ K/year, significant) was larger than the trend in nighttime temperature ($T_{\min, \text{trend}} = 0.033$ K/year, significant), resulting in a significant increasing DTR (0.014 K/year) (Fig. 2b, Table S1). During the NGS, DTR decreased significantly with -0.022 K/year because of opposite trends in T_{\max} and T_{\min} (Fig. 2c, Table S1).

3.2 Spatial heterogeneity of temperature trends

Spatial patterns of the temperature trends were generated from the 80 stations and MODIS LST product for all seasons (Figs. 3 and 4). Most of the stations showed significant warming in each season from 1982 to 2015. The warming rates displayed spatial heterogeneity between the northern TP (NTP) and the southern TP (STP), especially during the GS (the north and south are divided by Tanggula Mountains in this study). In the north, the warming rate of T_{mean} was generally higher than 0.04 K/year, while it was less than 0.04 K/year in the south. A common feature of the warming rate for each season was that the warming rate for T_{\max} was less than that of T_{\min} on the western TP, and greater than T_{\min} on the eastern side. This resulted in a decreased DTR_{trend} from east to west.

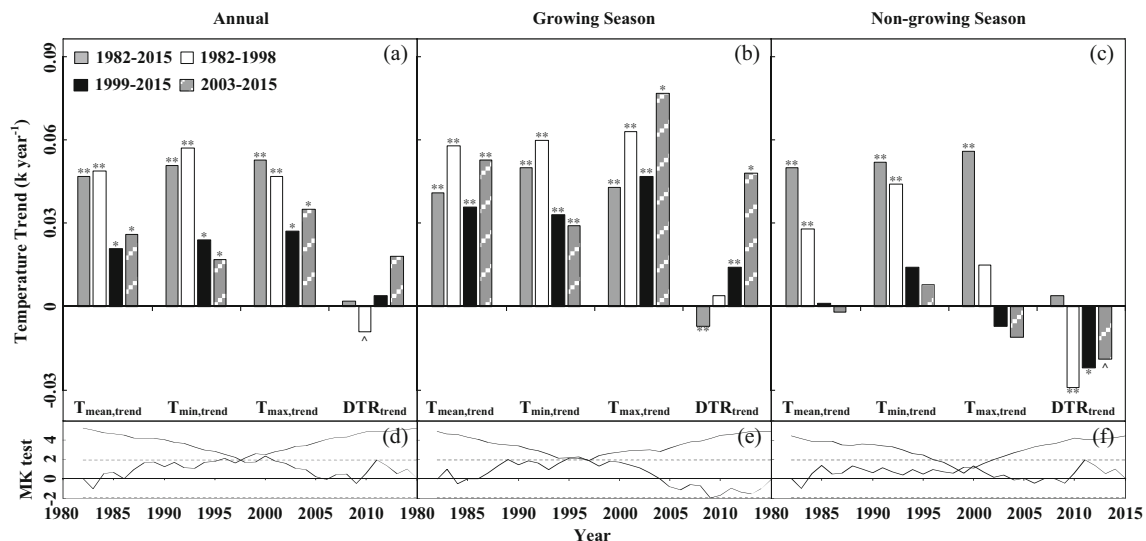


Fig. 2 Temperature trends of different time periods from 1982 to 2015. **a–c** Temperature trends of annual, growing season and non-growing season during 1982–2015, respectively. **d–f** Mann-Kendall tests of T_{mean} in annual, growing season and non-growing season, respectively and show the transitions in the trend. Grey columns represent the temperature trend from 1982 to 2015, white columns represent

temperature trend before 1998, black columns represent the temperature trend after 1998 and grey striped columns represent the MODIS LST trend from 2003 to 2015. In each panel, from left to right are $T_{\text{mean,trend}}$, $T_{\text{min,trend}}$, $T_{\text{max,trend}}$ and DTR_{trend} . p value smaller than 0.01 are expressed as **, p value smaller than 0.05 are expressed as * and p value smaller than 0.1 are expressed as ^

Consistent with the regional average, the spatial patterns of the temperature trends were locational exchange in north-south around 1998, especially during the GS. From 1982 to 1998, the annual, GS and NGS $T_{\text{mean,trend}}$ patterns were similar to 1982–2015, but more warming (more than 0.08 K/year) happened on the NTP in the first period. The DTR_{trend} pattern from 1982 to 1998, showing an increasing trend in the first period in the north and a decreasing trend on the STP, differed from that of 1982 to 2015. Both the remote sensing data (2003–2015) and the meteorological station data (1999–2015) showed however that the STP was still warming more than the NTP during the second period, especially for the daytime temperatures during the GS. The nighttime warming did not show any obvious spatial pattern, so that the DTR_{trend} was determined by daytime warming, increasing in the south and decreasing in the north during the GS.

3.3 Possible reasons for the temperature trends

Besides the change in temperature, other meteorological variables such as precipitation, sunshine duration, vapour pressure and wind speed, were also found to change (Fig. 5). On the TP, precipitation mainly falls during the GS, with an increasing but non-significant trend from 1982 to 2015. In the period before 1998, precipitation slightly increased, but a non-significant decrease was found after 1998. Sunshine duration, which was highly correlated with cloud amount, showed a significant decreasing trend from 1982 to 2015 (-0.006 h/year) and before 1998 (-0.018 h/year). However, the trend

slightly increased afterwards. Vapour pressure, the absolute content of water vapour in the air, showed a slightly increasing trend over the whole study period. This was composed of a steady rising trend (0.29 Pa/year) before 1998 and a significant declining trend (-0.278 Pa/year) after 1998. The average wind speed decreased significantly over the entire period (-0.13 m/s/year) from 1982 to 2015. This was due to a decrease before 1998 (-0.294 m/s/year) while it increased afterwards (0.095 m/s/year). All these results were found for the annual, GS and NGS periods.

Statistical analyses showed that there was no significant correlation between wind speed and temperature after detrending the original time series. The multivariate linear regression model (Table 1) showed that T_{mean} , T_{min} and T_{max} were all mostly affected by vapour pressure in all seasons. Sunshine duration was the second most important factor to act on temperature and mainly impacted T_{max} and DTR during the GS. The effect of precipitation on temperature was smallest among these three factors and mainly influenced DTR and T_{min} during the NGS.

For both the annual and GS periods, most areas showed a significant positive correlation between T_{min} and vapour pressure (Fig. 6). Several stations on the STP showed a negative correlation. The correlation between T_{max} and sunshine duration was significantly positive and was stronger in the south than in the north. The correlation between T_{mean} and vapour pressure had an obvious north-south pattern, being positive in the north and negative in the south. The correlation between DTR and sunshine duration was uniformly positive.

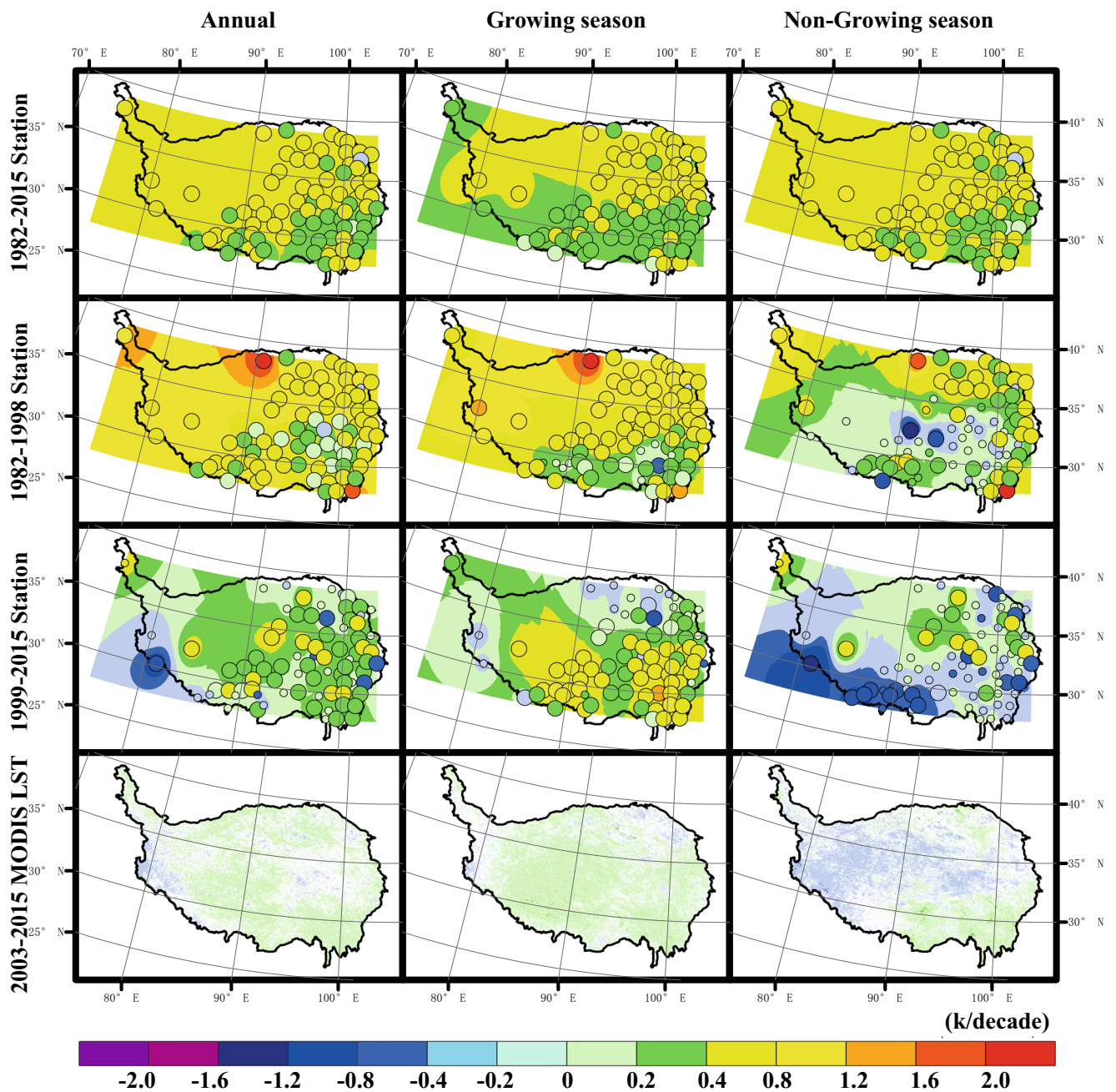


Fig. 3 Spatial patterns of $T_{\text{mean,trend}}$ in different periods over the TP. The p value is used for significance of the trend. Large circles and colourful pixels indicate a significant trend or $p < 0.1$

4 Discussion

4.1 The warming slowdown (or hiatus) over the TP

The first study that detected a warming hiatus at a global scale covered a period of 34 years from 1975 to 2008. The breaking point was found to be close to 1998 (Easterling and Wehner 2009). Follow-up research mainly used temperature records starting around 1980 (Gao et al. 2014; Santer et al. 2014; Solomon et al. 2010), around 1970 (Ding et al. 2014; Trenberth et al. 2014), or even earlier (Kosaka and Xie 2013), but all ended around 2010.

All studies found a hiatus or temperature slowdown around 1998. The present study targeted the period from 1982 to 2015 and also found a temperature hiatus around 1998 (Fig. 2, Fig. S1).

Interestingly, the first study detecting a hiatus over the TP suggested an absence of such a hiatus from 1998 to 2013. This was based on meteorological records (Duan and Xiao 2015). Two other studies, from 1999 to 2012 and from 2001 to 2015, neither suggested a warming hiatus (Cai et al. 2017; You et al. 2016). The contrasting findings may be due to the slightly different periods used. The starting and ending years may have been of great importance.

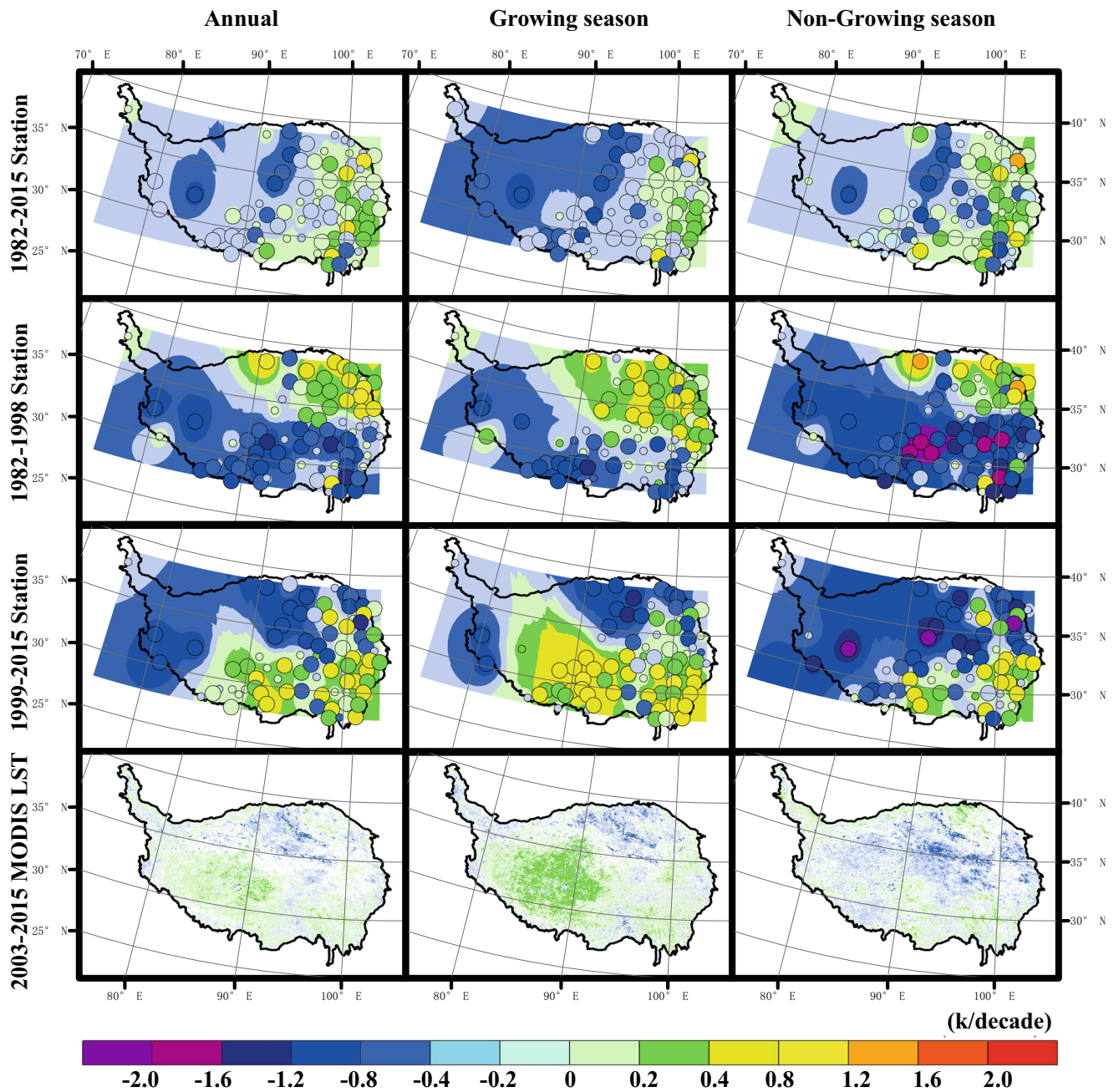


Fig. 4 Spatial patterns of DTR_{trend} in different periods over the TP. The p value is used for significance of the trend. Large circles and colourful pixels indicate a significant trend or $p < 0.1$

Besides the study period, the dataset seemed to have an influence on the results as well. You et al. found no hiatus over the TP, but only used the data of five meteorological stations at an elevation higher than 4500 m (You et al. 2016). The research of Cai et al. and Duan and Xiao both included several meteorological stations in the southern Hengduan Mountain region (Cai et al. 2017; Duan and Xiao 2015), which were not used in our study. The same studies also excluded the southern part of the Xinjiang Autonomous Region from the TP, and figured out the result based on the only two stations data over the vast west TP (Cai et al. 2017;

Duan and Xiao 2015). Consequently, their findings are different from the present study.

Furthermore, satellite-derived LST data from both Terra (Cai et al. 2017; Qin et al. 2009) and Aqua (Tao et al. 2014; Xu et al. 2013; Zhang et al. 2016a, b) can be used. Terra has a slightly longer duration of 2 years starting from 2001 instead of 2003. However, compared to Terra, Aqua had a more adequate overpass time of 0130 hours and 1330 hours, close to the daily T_{min} and T_{max} . Moreover, remotely sensed temperature data is strongly affected by clouds, especially on the TP (Xu et al. 2013; Zhang et al. 2016b). To obtain reliable results,

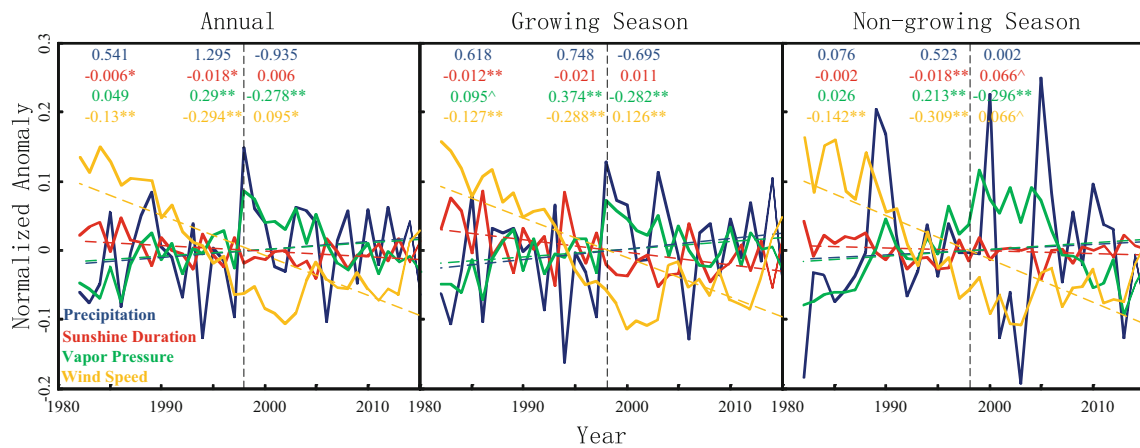


Fig. 5 Observed annual mean anomalies of precipitation, sunshine duration, vapour pressure and wind speed over the TP for the period of 1982–2015. The units of precipitation, sunshine duration, vapour

pressure and wind speed are millimetre per year, hour per year, Pascal per year and miles per second per year, respectively

we used the HANTS algorithm (Section 2.2), interpolating the satellite-derived LST data (Xu et al. 2013).

The method of calculating the warming rates may also have played a role in the different results. We used the Mann-Kendall trend test, as in Ding et al., rather than an artificially based decision (Cai et al. 2017; Ding et al. 2014; Duan and Xiao 2015). The Mann-Kendall test is a non-parametric test

that requires the data to be independent but it does not need to be normally distributed (Kendall 1955; Mann 1945). Furthermore, we used a linear regression after applying a 5-year moving average to reduce the effects of interannual fluctuations. Other studies used a simple linear regression model without pretreatment of the data (Cai et al. 2017) or a Sen’s slope after Mann-Kendall test (You et al. 2016).

Table 1 Statistical relationships between changes in temperature and changes in precipitation, sunshine duration, and vapour pressure over the TP

Period	Y	$Y = \beta_0 + \beta_1 P + \beta_2 S + \beta_3 V + \beta_4 \text{time} + \varepsilon$			
		R^2	β_1	β_2	β_3
Annual	T_{mean}	0.256	0.001	0.968	0.107**
	T_{min}	0.317	0.002	0.125	0.082*
	T_{max}	0.272	0.001	1.952*	0.13**
	DTR	0.644	-0.001	1.864**	0.051*
GS	T_{mean}	0.475	0	0.861**	0.092**
	T_{min}	0.461	0.001	0.238	0.083**
	T_{max}	0.526	0	1.445**	0.1**
	DTR	0.783	-0.003^	1.052**	0.02
NGS	T_{mean}	0.371	0.008	2.363**	0.162**
	T_{min}	0.352	0.017*	1.498*	0.13**
	T_{max}	0.468	0.001	3.607**	0.198**
	DTR	0.684	-0.016**	2.036**	0.072*

Regression coefficients, β_0 (not shown), β_1 , β_2 , β_3 and linear time trends, β_4 (shown in Fig. 2), with ^, * and ** are statistically significant at the 90, 95 and 99% level, respectively. A two-tailed Student’s *t* test was used to test whether β_1 or β_2 or β_3 or β_4 differs significantly from zero. To avoid spurious regressions, detrending the original time series was used to estimate relationships between changes in temperature and changes in precipitation, sunshine duration and vapour pressure

P precipitation (mm/year), *S* sunshine duration (hour/day), *V* vapour pressure (Pa), T_{mean} mean temperature (K), T_{max} maximum temperature (K), T_{min} minimum temperature (K), *DTR* diurnal temperature range (K)

4.2 Possible reasons for the warming slowdown (or hiatus) and its spatial pattern

The global warming hiatus is extensively studied and different factors have been found to play a role, such as water vapour (Solomon et al. 2010), clouds (Mauritsen 2016), aerosols (Santer et al. 2014), an imbalance of energy at the top of the atmosphere (Hedemann et al. 2017) and effects of the ocean (Guemas et al. 2013). Over China, this warming hiatus has also been observed in, for example, a homogenized meteorological dataset and reanalyses data (Li et al. 2015; Xie et al. 2017). Possible reasons for the warming slowdown here have been suggested to be decreasing downward shortwave radiation (Li et al. 2015) and changes in the large-scale circulation (Xie et al. 2017). We showed that over the TP, as in (Duan and Xiao 2015), wind speed, sunshine duration, vapour pressure and precipitation, all variables related to temperature, reversed their trends in 1998.

Wind stilling was thought to be responsible for the rapid warming over the TP since the 1980s (Yang et al. 2014). However, we did not find a significant correlation between wind speed and temperature after detrending the time series. The reduced wind speed may have been caused by a weakening surface pressure gradient between high and low latitudinal regions due to a latitudinal difference of global warming (Yang et al. 2012) and may have been a coincidence rather than a driving factor behind the regional warming. The prominent trend in winter warming over the TP could be a result of

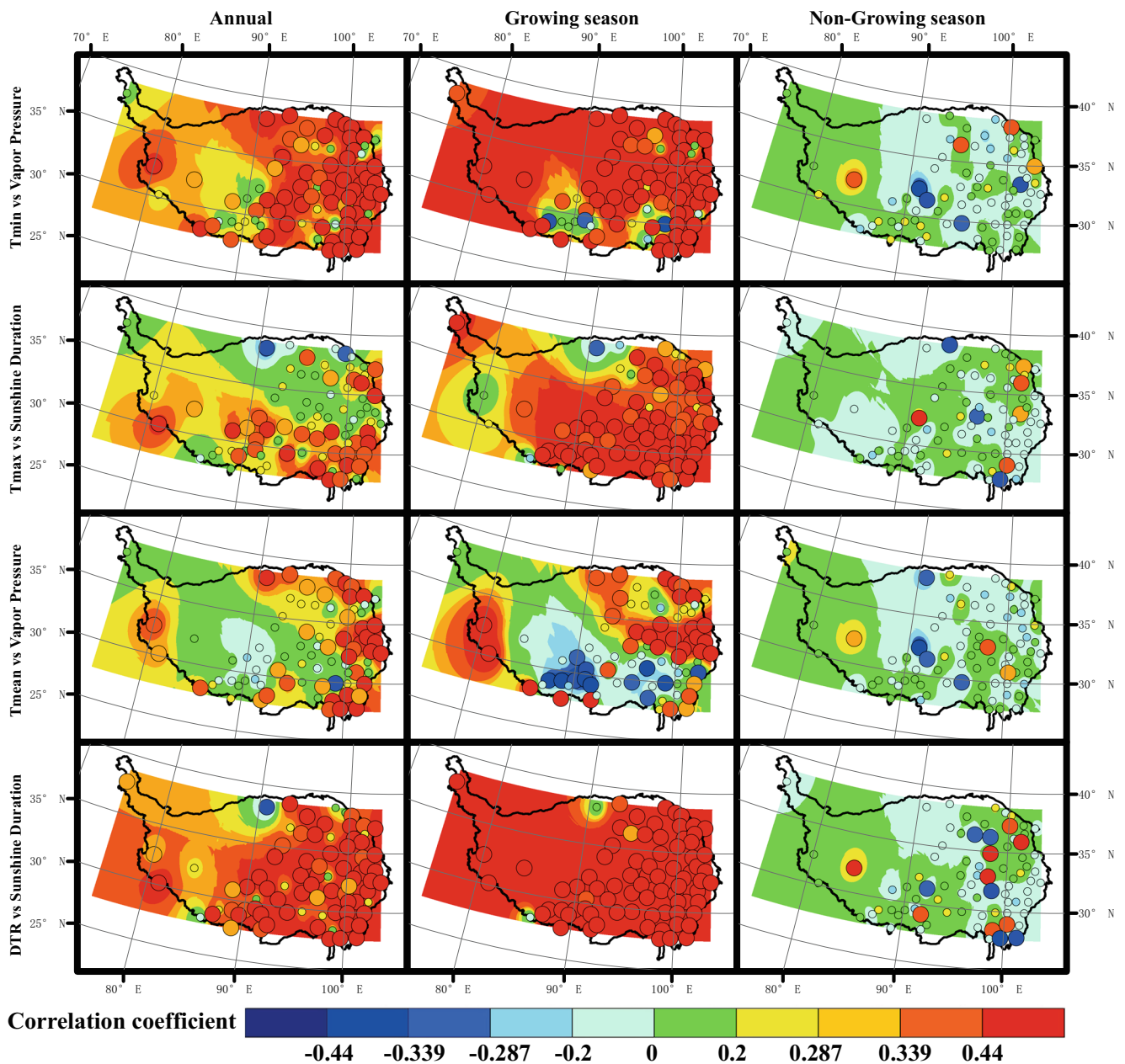


Fig. 6 Spatial pattern of the correlation between temperature and its driving force; ± 0.287 , ± 0.339 and ± 0.44 are statistically significant at the 90, 95, and 99% level, respectively

enhanced downward long wave radiation caused by increased surface water vapour (Rangwala et al. 2009). This was confirmed by our study, especially for nighttime temperature. Increased sunshine duration can also contribute to temperature increase (Wang et al. 2014). Also, this finding was supported by our study and was especially clear for T_{\max} . The variation of incoming solar radiation shows a decadal variability similar to sunshine duration (Yang et al. 2014). It has been suggested that enhanced precipitation in the STP accompanied by higher low-cloud cover may have slowed the warming by decreasing the incoming shortwave

radiation and increasing the latent heat flux (Duan et al. 2015). We found a positive relation between precipitation and nighttime temperature during the NGS, which may have been due to the increasing downward long wave radiation from low-level clouds that are capable of producing precipitation.

The warming trend over the TP showed spatial heterogeneity. We found more warming in the north than the south, especially in the GS, from 1982 to 2015. The largest difference in the warming between the north and the south was 0.70 ± 0.11 K during the summer (June–August), while the smallest

difference was 0.27 ± 0.14 K during the cold season (November–April) from 1984 to 2013 (Duan et al. 2015). This stems from a larger warming rate at stations in the central TP during the dry (cold) season than in the wet (warm) season (Gao et al. 2015). This north-south difference could also be due to pollution emissions from industrial processes (i.e. brown clouds) and urbanization. The dominant weakening of the zonal wind speed over the TP resulted from global warming and ozone depletion ratios (Guo and Wang 2012; Wang et al. 2014).

Interestingly, the north-south spatial pattern of temperature change also reversed in 1998. This was also found by previous studies (Cai et al. 2017; Tao et al. 2014). Water vapour and sunshine duration, two major driving factors, had a trade-off effect on temperature. Water vapour enhanced the downward long wave radiation at nighttime and thereby the nighttime warming, while sunshine duration increased the downward shortwave radiation at daytime, causing daytime warming. So, the mean effect seems to be the consequence of water vapour and sunshine duration together. Over the NTP, the nighttime warming caused by water vapour was larger than the daytime cooling induced by decreasing sunshine duration, resulting in a positive correlation between T_{mean} and water vapour. Over the STP, the magnitude of the daytime warming caused by increased sunshine duration was larger than the magnitude of the nighttime cooling caused by decreasing water vapour. Thus, water vapour and sunshine duration were the main reasons for T_{mean} warming in the NTP and STP, respectively.

Acknowledgments We thank Jian Tao, Tao Zhang, Yi Xi, Jyoti Bhandari, Ze Tang, Junxiang Li and Yixuan Zhu for their valuable comments and suggestions. We also thank the journal editor and the anonymous reviewers for their useful comments and efforts on this paper.

Funding This research was funded by the following projects: the Chinese National Key Program for Developing Basic Science (2013CB956302) and the Science and Technology Project of the Chinese Academy of Sciences (XDA05050400).

References

- An ZS, Kutzbach JE, Prell WL, Porter SC (2001) Evolution of Asian monsoons and phased uplift of the Himalayan Tibetan plateau since late Miocene times. *Nature* 411:62–66
- An WL, Hou SG, Zhang WB, Wu SY, Xu H, Pang HX, Wang YT, Liu YP (2016) Possible recent warming hiatus on the northwestern Tibetan plateau derived from ice core records. *Sci Rep* 6:8
- Cai DL, You QL, Fraedrich K, Guan YN (2017) Spatiotemporal temperature variability over the Tibetan plateau: altitudinal dependence associated with the global warming hiatus. *J Clim* 30:969–984
- Cowtan K, Way RG (2014) Coverage bias in the HadCRUT4 temperature series and its impact on recent temperature trends. *Q J R Meteorol Soc* 140:1935–1944
- Ding M, Li L, Zhang Y, Liu L, Wang Z (2014) Temperature change and its elevation dependency on the Tibetan plateau and its vicinity from 1971 to 2012. *Resour Sci* 36:1509–1518
- Duan AM, Xiao ZX (2015) Does the climate warming hiatus exist over the Tibetan plateau? *Sci Rep* 5:9
- Duan JP, Li L, Fang YJ (2015) Seasonal spatial heterogeneity of warming rates on the Tibetan plateau over the past 30 years. *Sci Rep* 5:8
- Easterling DR, Wehner MF (2009) Is the climate warming or cooling? *Geophys Res Lett* 36:3
- Fyfe JC, Gillett NP, Zwiers FW (2013a) Overestimated global warming over the past 20 years. *Nat Clim Chang* 3:767–769
- Fyfe JC, von Salzen K, Cole JNS, Gillett NP, Vernier JP (2013b) Surface response to stratospheric aerosol changes in a coupled atmosphere-ocean model. *Geophys Res Lett* 40:584–588
- Fyfe JC, Meehl GA, England MH, Mann ME, Santer BD, Flato GM, Hawkins E, Gillett NP, Xie SP, Kosaka Y, Swart NC (2016) Making sense of the early-2000s warming slowdown. *Nat Clim Chang* 6:224–228
- Gao YH, Cuo L, Zhang YX (2014) Changes in moisture flux over the Tibetan plateau during 1979–2011 and possible mechanisms. *J Clim* 27:1876–1893
- Gao YH, Xu JW, Chen DL (2015) Evaluation of WRF mesoscale climate simulations over the Tibetan plateau during 1979–2011. *J Clim* 28:2823–2841
- Guemas V, Doblas-Reyes FJ, Andreu-Burillo I, Asif M (2013) Retrospective prediction of the global warming slowdown in the past decade. *Nat Clim Chang* 3:649–653
- Guo DL, Wang HJ (2012) The significant climate warming in the northern Tibetan plateau and its possible causes. *Int J Climatol* 32:1775–1781
- Haywood JM, Jones A, Jones GS (2014) The impact of volcanic eruptions in the period 2000–2013 on global mean temperature trends evaluated in the HadGEM2-ES climate model. *Atmos Sci Lett* 15:92–96
- Hedemann C, Mauritsen T, Jungclaus J, Marotzke J (2017) The subtle origins of surface-warming hiatuses. *Nat Clim Chang* 7:336–339
- IPCC (2013) Summary for policymakers. In *Climate Change 2013: The physical science basis. Working Group I to the Fifth Assessment Report of the Intergovernmental Panel on Climate Change*
- Karl TR, Arguez A, Huang BY, Lawrimore JH, McMahon JR, Menne MJ, Peterson TC, Vose RS, Zhang HM (2015) Possible artifacts of data biases in the recent global surface warming hiatus. *Science* 348:1469–1472
- Kaufmann RK, Kauppi H, Mann ML, Stock JH (2011) Reconciling anthropogenic climate change with observed temperature 1998–2008. *Proc Natl Acad Sci U S A* 108:11790–11793
- Kendall MG (1955) Rank correlation methods. Charles Griffin, London
- Kosaka Y, Xie SP (2013) Recent global-warming hiatus tied to equatorial Pacific surface cooling. *Nature* 501:403–407
- Li QX, Yang S, Xu WH, Wang XLL, Jones P, Parker D, Zhou LM, Feng Y, Gao Y (2015) China experiencing the recent warming hiatus. *Geophys Res Lett* 42:889–898
- Liu XD, Cheng ZG, Yan LB, Yin ZY (2009) Elevation dependency of recent and future minimum surface air temperature trends in the Tibetan plateau and its surroundings. *Glob Planet Chang* 68:164–174
- Mann HB (1945) Nonparametric tests against trend. *Econometrica* 13:245–259
- Mauritsen T (2016) Global warming clouds cooled the earth. *Nat Geosci* 9:865–867
- Mears CA, Wentz FJ, Thorne P, Bernie D (2011) Assessing uncertainty in estimates of atmospheric temperature changes from MSU and AMSU using a Monte-Carlo estimation technique. *J Geophys Res-Atmos* 116:16
- Meehl GA, Arblaster JM, Fasullo JT, Hu AX, Trenberth KE (2011) Model-based evidence of deep-ocean heat uptake during surface-temperature hiatus periods. *Nat Clim Chang* 1:360–364
- Morice CP, Kennedy JJ, Rayner NA, Jones PD (2012) Quantifying uncertainties in global and regional temperature change using an

- ensemble of observational estimates: the HadCRUT4 data set. *J Geophys Res-Atmos* 117:22
- Naud CM, Miller JR, Landry C (2012) Using satellites to investigate the sensitivity of longwave downward radiation to water vapor at high elevations. *J Geophys Res-Atmos* 117:12
- Pepin N, Bradley RS, Diaz HF, Baraer M, Caceres EB, Forsythe N, Fowler H, Greenwood G, Hashmi MZ, Liu XD, Miller JR, Ning L, Ohmura A, Palazzi E, Rangwala I, Schonert W, Severskiy I, Shahgedanova M, Wang MB, Williamson SN, Yang DQ, Mt Res Initiative EDWWG (2015) Elevation-dependent warming in mountain regions of the world. *Nat Clim Chang* 5:424–430
- Piao SL, Tan K, Nan HJ, Ciais P, Fang JY, Wang T, Vuichard N, Zhu BA (2012) Impacts of climate and CO₂ changes on the vegetation growth and carbon balance of Qinghai-Tibetan grasslands over the past five decades. *Glob Planet Chang* 98–99:73–80
- Qin J, Yang K, Liang SL, Guo XF (2009) The altitudinal dependence of recent rapid warming over the Tibetan plateau. *Clim Chang* 97:321–327
- Rangwala I, Miller JR, Xu M (2009) Warming in the Tibetan plateau: possible influences of the changes in surface water vapor. *Geophys Res Lett* 36:6
- Rangwala I, Miller JR, Russell GL, Xu M (2010) Using a global climate model to evaluate the influences of water vapor, snow cover and atmospheric aerosol on warming in the Tibetan plateau during the twenty-first century. *Clim Dyn* 34:859–872
- Roerink GJ, Menenti M, Verhoef W (2000) Reconstructing cloudfree NDVI composites using Fourier analysis of time series. *Int J Remote Sens* 21:1911–1917
- Ruckstuhl C, Philipona R, Morland J, Ohmura A (2007) Observed relationship between surface specific humidity, integrated water vapor, and longwave downward radiation at different altitudes. *J Geophys Res-Atmos* 112:7
- Santer BD, Bonfils C, Painter JF, Zelinka MD, Mears C, Solomon S, Schmidt GA, Fyfe JC, Cole JNS, Nazarenko L, Taylor KE, Wentz FJ (2014) Volcanic contribution to decadal changes in tropospheric temperature. *Nat Geosci* 7:185–189
- Smith DM, Booth BBB, Dunstone NJ, Eade R, Hermanson L, Jones GS, Scaife AA, Sheen KL, Thompson V (2016) Role of volcanic and anthropogenic aerosols in the recent global surface warming slowdown. *Nat Clim Chang* 6:936–940
- Solomon S, Rosenlof KH, Portmann RW, Daniel JS, Davis SM, Sanford TJ, Plattner GK (2010) Contributions of stratospheric water vapor to decadal changes in the rate of global warming. *Science* 327:1219–1223
- Solomon S, Daniel JS, Neely RR, Vernier JP, Dutton EG, Thomason LW (2011) The persistently variable “background” stratospheric aerosol layer and global climate change. *Science* 333:866–870
- Tao J, Zhang YJ, Zhu JT, Jiang YB, Zhang XZ, Zhang T, Xi Y (2014) Elevation-dependent temperature change in the Qinghai-Xizang plateau grassland during the past decade. *Theor Appl Climatol* 117:61–71
- Tian L, Zhang YJ, Zhu JT (2014) Decreased surface albedo driven by denser vegetation on the Tibetan plateau. *Environ Res Lett* 9:11
- Trenberth KE, Fasullo JT, Branstator G, Phillips AS (2014) Seasonal aspects of the recent pause in surface warming. *Nat Clim Chang* 4: 911–916
- Tudoroiu M, Eccel E, Gioli B, Gianelle D, Schume H, Genesio L, Miglietta F (2016) Negative elevation-dependent warming trend in the eastern alps. *Environ Res Lett* 11:12
- Wan ZM, Dozier J (1996) A generalized split-window algorithm for retrieving land-surface temperature from space. *IEEE Trans Geosci Remote Sens* 34:892–905
- Wang XJ, Yang MX, Liang XW, Pang GJ, Wan GN, Chen XL, Luo XQ (2014) The dramatic climate warming in the Qaidam Basin, north-eastern Tibetan plateau, during 1961–2010. *Int J Climatol* 34:1524–1537
- Xie YK, Huang JP, Liu YZ (2017) From accelerated warming to warming hiatus in China. *Int J Climatol* 37:1758–1773
- Xu YM, Shen Y, Wu ZY (2013) Spatial and temporal variations of land surface temperature over the Tibetan plateau based on harmonic analysis. *Mt Res Dev* 33:85–94
- Yan LB, Liu ZY, Chen GS, Kutzbach JE, Liu XD (2016) Mechanisms of elevation-dependent warming over the Tibetan plateau in quadrupled CO₂ experiments. *Clim Chang* 135:509–519
- Yang XM, Li ZX, Feng Q, He YQ, An WL, Zhang W, Cao WH, Yu TF, Wang YM, Theakstone WH (2012) The decreasing wind speed in southwestern China during 1969–2009, and possible causes. *Quat Int* 263:71–84
- Yang K, Wu H, Qin J, Lin CG, Tang WJ, Chen YY (2014) Recent climate changes over the Tibetan plateau and their impacts on energy and water cycle: a review. *Glob Planet Chang* 112:79–91
- You QL, Fraedrich K, Ren GY, Pepin N, Kang SC (2013) Variability of temperature in the Tibetan plateau based on homogenized surface stations and reanalysis data. *Int J Climatol* 33:1337–1347
- You QL, Min JZ, Kang SC (2016) Rapid warming in the Tibetan plateau from observations and CMIP5 models in recent decades. *Int J Climatol* 36:2660–2670
- Zeng ZZ, Chen AP, Ciais P, Li Y, Li LZ, Vautard R, Zhou LM, Yang H, Huang MT, Piao SL (2015) Regional air pollution brightening reverses the greenhouse gases induced warming-elevation relationship. *Geophys Res Lett* 42:4563–4572
- Zhang Y, Li B, Zheng D (2002) A discussion on the boundary and area of the Tibetan plateau in China. *Geogr Res* 21:1–8
- Zhang GL, Zhang YJ, Dong JW, Xiao XM (2013) Green-up dates in the Tibetan plateau have continuously advanced from 1982 to 2011. *Proc Natl Acad Sci U S A* 110:4309–4314
- Zhang HB, Zhang F, Ye M, Che T, Zhang GQ (2016a) Estimating daily air temperatures over the Tibetan plateau by dynamically integrating MODIS LST data. *J Geophys Res-Atmos* 121:11425–11441
- Zhang HB, Zhang F, Zhang GQ, He XB, Tian LD (2016b) Evaluation of cloud effects on air temperature estimation using MODIS LST based on ground measurements over the Tibetan plateau. *Atmos Chem Phys* 16:13681–13696
- Zhong L, Su ZB, Ma YM, Salama MS, Sobrino JA (2011) Accelerated changes of environmental conditions on the Tibetan plateau caused by climate change. *J Clim* 24:6540–6550
- Zhou LM, Dickinson RE, Tian YH, Vose RS, Dai YJ (2007) Impact of vegetation removal and soil aridation on diurnal temperature range in a semiarid region: application to the Sahel. *Proc Natl Acad Sci U S A* 104:17937–17942